

Tau lepton physics at Belle

Kiyoshi Hayasaka (KMI, Nagoya U.)

Furo-cho, Chikusa-ku, Nagoya, Japan

E-mail: hayasaka@hepl.phys.nagoya-u.ac.jp

Abstract. We report the recent results of a search for lepton-flavor-violating τ decays and a search for CP violation in τ to $\nu K_S^0 \pi$ using a large data sample accumulated with the Belle detector at the KEKB asymmetric-energy e^+e^- collider. The sensitivity to these modes is significantly improved compared to previous experiments.

1. Introduction

The success of the B-factory provides us the world-largest data sample of $\tau^+\tau^-$ -pairs, that is useful for a search for New Physics (NP). Here, we discuss new phenomena relating to τ decays, in particular, lepton-flavor-violating τ decays and CP violation in a τ decay using an around 1 ab^{-1} data sample accumulated with the Belle detector at the KEKB asymmetric-energy e^+e^- collider,

An observation of the charged-lepton-flavor violation (cLFV) is a clear signature of NP since the cLFV has a negligibly small probability in the Standard Model (SM) even taking into account neutrino oscillations and many of models for NP naturally predict cLFV. In particular, lepton-flavor-violating (LFV) τ decays are allowed to have various kinds of final states and some of them are expected to have a measurably large branching fraction, depending on the models. Therefore, not only to find the NP phenomenon but to distinguish the models, it is important to search for the LFV τ decays.

Similarly to the LFV τ decays, an observation of CP violation (CPV) in a τ decay is also a clear signature of NP. Here, we focus on the CPV in a τ decay into $\nu K_S^0 \pi$ induced by a new scalar particle such as a charged Higgs in a multi-Higgs-doublet model. This kind of CPV can be observed as a difference in the τ^\pm decay angular distributions by the interference effect between the scalar and (axial-)vector components of the intermediate state in the decay.

2. $\tau \rightarrow \ell M^0$ ($\ell = e, \mu$, $M^0 = \pi^0, \eta, \eta', \rho^0, K^{*0}, \bar{K}^{*0}, \omega$ and ϕ)

Generally, $\tau \rightarrow \mu \gamma$ is the most promising among various LFV τ decays in many models for NP. However, in some models, such as non-universal-Higgs-mass model [1], $\tau \rightarrow \mu \eta$ can have the largest branching fraction. In addition, a magnitude relation among the branching fractions for the LFV τ decays will help to distinguish the NP models. Here, we show the results for the two-body τ decays into a lepton and a neutral meson (pseudoscalar and vector).

2.1. Analysis Method

In the LFV τ analysis, in order to evaluate the number of signal events, two independent variables are defined, that are signal-reconstructed mass and energy in the center-of-mass (CM) frame

from energies and momenta for the signal τ daughters. In the $\tau \rightarrow \mu\eta$ case, they are defined as

$$M_{\mu\eta} = \sqrt{E_{\mu\eta}^2 - P_{\mu\eta}^2}, \quad (1)$$

$$\Delta E = E_{\mu\eta}^{\text{CM}} - E_{\text{beam}}^{\text{CM}}, \quad (2)$$

where $E_{\mu\eta}$ ($P_{\mu\eta}$) is a sum of the energies (a magnitude of a vector sum of the momenta) for μ and η , the superscript CM indicates that the variable is defined in the CM frame and the $E_{\text{beam}}^{\text{CM}}$ means the initial beam energy in the CM frame. Principally, $M_{\mu\eta}$ and ΔE are expected to be m_τ ($\sim 1.78 \text{ GeV}/c^2$) and 0 (GeV), respectively, for signal events while $M_{\mu\eta}$ and ΔE will smoothly vary without any special structure in the background (BG) events. The signal MC distribution of $\tau \rightarrow \mu\eta$ on the $M_{\mu\eta} - \Delta E$ plane is shown in Fig. 1. Due to the resolution, the

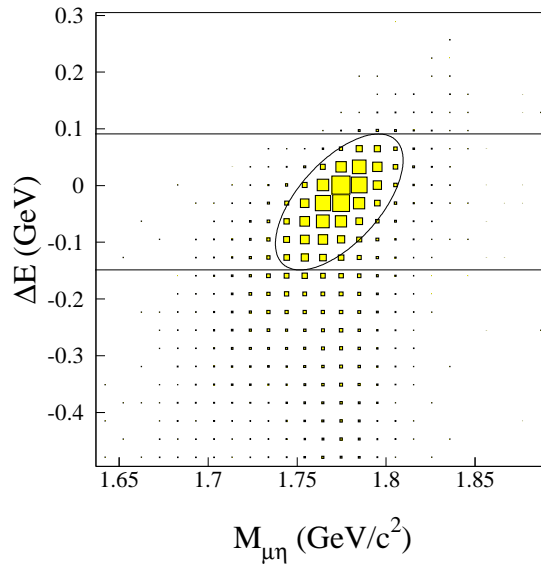


Figure 1. Distribution for the $\tau \rightarrow \mu\eta$ signal events. An elliptical region is defined as a signal region, that corresponds to $\pm 3\sigma$ and a region between two parallel lines excluding the signal region is used for the BG estimation as a sideband region, where the resolution σ is evaluated by a asymmetric-Gaussian fit to the signal MC distribution.

signal events are distributed around $M_{\mu\eta} \sim m_\tau$ and $\Delta E \sim 0$ (GeV). Taking into account the resolution, we set the elliptic signal region. (See Fig. 1.) Since the resolution for the photon energy is not so good as that for the momentum of the charged track, the signal region of the mode having some photons in the final state can be large.

To avoid any bias for our analyses, we perform the blind analysis, i.e., we do not observe the data events in the signal region before fixing the selection criteria and the evaluation for the systematic uncertainties and the expected number of the BG events. Finally, we observe some signal events or evaluate an upper limit of the number of the signal event at 90% confidence level (CL) using the expected number of the BG event and the number of the observed events in the signal region by Feldman-Cousins approach. [2]

Table 1. Summary for the efficiency (Eff.), the expected number of the BG events, (N_{BG}^{exp}) and the upper limit on the branching fraction (UL) for each mode, where “comb.” means the combined result from subdecay modes.

Mode ($\tau \rightarrow$)	Eff.(%)	N_{BG}^{exp}	UL ($\times 10^{-8}$)	Mode ($\tau \rightarrow$)	Eff.(%)	N_{BG}^{exp}	UL ($\times 10^{-8}$)
$\mu\eta(\rightarrow \gamma\gamma)$	8.2	0.63 ± 0.37	3.6	$e\eta(\rightarrow \gamma\gamma)$	7.0	0.66 ± 0.38	8.2
$\mu\eta(\rightarrow \pi\pi\pi^0)$	6.9	0.23 ± 0.23	8.6	$e\eta(\rightarrow \pi\pi\pi^0)$	6.3	0.69 ± 0.40	8.1
$\mu\eta(\text{comb.})$			2.3	$e\eta(\text{comb.})$			4.4
$\mu\eta'(\rightarrow \pi\pi\eta)$	8.1	$0.00^{+0.16}_{-0.00}$	10.0	$e\eta'(\rightarrow \pi\pi\eta)$	7.3	0.63 ± 0.45	9.4
$\mu\eta'(\rightarrow \gamma\rho^0)$	6.2	0.59 ± 0.41	6.6	$e\eta'(\rightarrow \gamma\rho^0)$	7.5	0.29 ± 0.29	6.8
$\mu\eta'(\text{comb.})$			3.8	$e\eta'(\text{comb.})$			3.6
$\mu\pi^0$	4.2	0.64 ± 0.32	2.7	$e\pi^0$	4.7	0.89 ± 0.40	2.2

2.2. $\tau \rightarrow \ell P^0$ ($\ell = e, \mu$, $P^0 = \pi^0, \eta, \eta'$)

We perform a new search for the τ decay into a lepton (e or μ) and a neutral pseudoscalar (π^0 , η or η') with a 901 fb^{-1} data sample, that corresponds to 8.2×10^8 $\tau^+\tau^-$ -pairs. A neutral pion is reconstructed from 2 photons while an η (η') is reconstructed from $\gamma\gamma$ ($\rho^0\gamma$) as well as $\pi^+\pi^-\pi^0$ ($\pi^+\pi^-\eta$) to increase the detection efficiency. When the neutral pseudoscalars are reconstructed, their four-momentum is evaluated by a mass-constrained fit to obtain a better resolution for the signal region. Because we have modified the selection criteria applied to the previous analysis, we obtain an about 1.5 times better detection efficiency while a similar background level is kept. Here, the number of the BG events in the signal region is evaluated by an interpolation from the number of the observed events in the sideband region, assuming a flat distribution for the BG events in the signal and sideband region.

As a result, we observe one event in the $\tau \rightarrow e\eta(\rightarrow \gamma\gamma)$ mode while no events are found in other modes as shown in Fig. 2. Since these results are consistent with the background estimation, we set upper limits on the following branching fractions, as shown in Table 1. Consequently, we

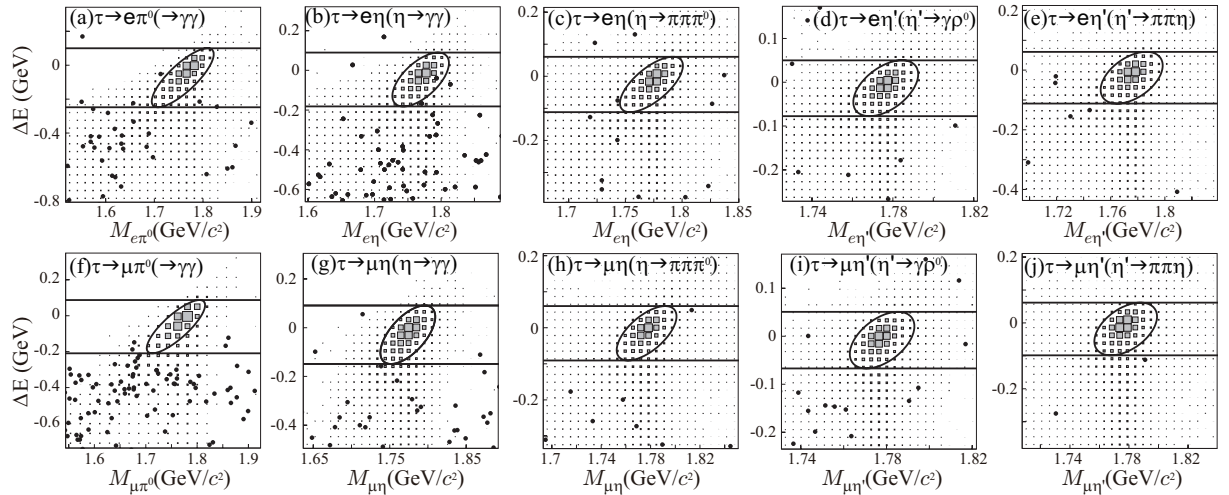


Figure 2. Resulting 2D plots for $\tau \rightarrow e\pi^0$ (a), $e\eta(\rightarrow \gamma\gamma)$ (b), $e\eta(\rightarrow \pi\pi\pi^0)$ (c), $e\eta'(\rightarrow \gamma\rho^0(\rightarrow \pi\pi))$ (d), $e\eta'(\rightarrow \pi\pi\eta(\rightarrow \gamma\gamma))$ (e), $\mu\pi^0$ (f), $\mu\eta(\rightarrow \gamma\gamma)$ (g), $\mu\eta(\rightarrow \pi\pi\pi^0)$ (h), $\mu\eta'(\rightarrow \gamma\rho^0(\rightarrow \pi\pi))$ (i) and $\mu\eta'(\rightarrow \pi\pi\eta(\rightarrow \gamma\gamma))$ (j), on the $M_{\ell P^0} - \Delta E$ plane. Here, black dots (shaded boxes) express the data (signal MC), the region bounded by two lines is defined as a 3σ band for the BG estimation and the elliptic region is the signal one which corresponds to 3σ in each plot. One event is found in the signal region for $\tau \rightarrow e\eta$ while no events appear in any other modes.

Table 2. Summary for the efficiency (Eff.), the expected number of the BG events, (N_{BG}^{exp}) and the upper limit on the branching fraction (UL) for each mode.

Mode ($\tau \rightarrow$)	Eff.(%)	N_{BG}^{exp}	UL ($\times 10^{-8}$)	Mode ($\tau \rightarrow$)	Eff.(%)	N_{BG}^{exp}	UL ($\times 10^{-8}$)
$\mu\rho^0$	7.1	1.48 ± 0.35	1.2	$e\rho^0$	7.6	0.29 ± 0.15	1.8
μK^{*0}	3.4	0.53 ± 0.20	7.2	$e K^{*0}$	4.4	0.39 ± 0.14	3.2
$\mu \bar{K}^{*0}$	3.6	0.45 ± 0.17	7.0	$e \bar{K}^{*0}$	4.4	0.08 ± 0.08	3.4
$\mu\omega$	2.4	0.72 ± 0.18	4.7	$e\omega$	2.9	0.30 ± 0.14	4.8
$\mu\phi$	3.2	0.06 ± 0.06	8.4	$e\phi$	4.2	0.47 ± 0.19	3.1

obtain a (2.1 – 4.4) times more sensitive result than previously.

2.3. $\tau \rightarrow \ell V^0$ ($\ell = e, \mu$, $V^0 = \rho^0, K^{*0}, \bar{K}^{*0}, \omega, \phi$)

Similarly to $\tau^- \rightarrow \ell^- P^0$, we update our results of the search for $\tau^- \rightarrow \ell^- V^0$, where $\ell = e, \mu$, $V^0 = \rho^0, K^{*0}, \bar{K}^{*0}, \omega, \phi$ with an 854 fb^{-1} data sample, that corresponds to 7.8×10^8 $\tau^+\tau^-$ pairs [3]. Here, $\rho^0, K^{*0}, \bar{K}^{*0}, \omega$ and ϕ are reconstructed from $\pi^+\pi^-$, π^-K^+ , π^+K^- , $\pi^+\pi^-\pi^0$ and K^+K^- , respectively. By performing a detailed background study, we obtain a 1.2 times better efficiency in average with keeping similar level backgrounds. For the modes including a μ , BG events mainly come from $\tau\tau$ events while some two-photon process or radiative Bhabha process with a gamma conversion becomes main background in the modes having an electron. Finally, one event is found in the signal region for $\tau^- \rightarrow \mu^- K^{*0}$, $\mu^- \bar{K}^{*0}$ and $\mu^- \phi$ while no events appear in any other modes. (See Fig. 3.) They are consistent with the expected number of the backgrounds. Consequently, we set the 90% confidence level upper limits on the branching fractions as shown in Table 2. At the present, the upper limit for $\tau \rightarrow \mu\rho^0$ is the most sensitive among the all LFV τ decays. (See Fig. 4, where all of the current upper limits are shown.)

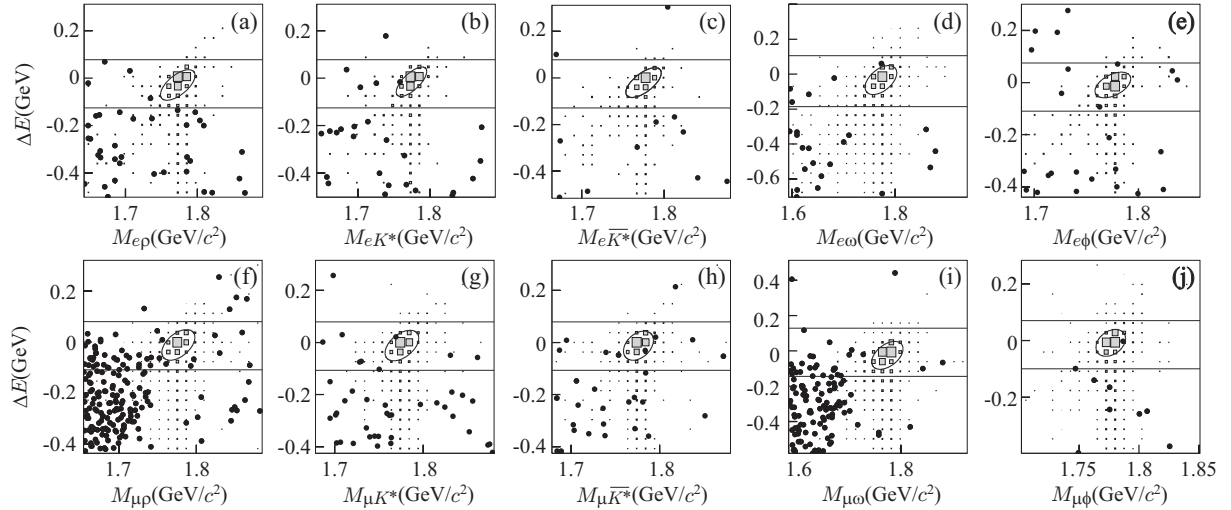


Figure 3. Resulting 2D plots for $\tau \rightarrow e\rho^0$ (a), eK^{*0} (b), $e\bar{K}^{*0}$ (c), $e\omega$ (d), $e\phi$ (e), $\mu\rho^0$ (f), μK^{*0} (g), $\mu\bar{K}^{*0}$ (h), $\mu\omega$ (i) and $\mu\phi$ (j) on the $M_{\ell V^0} - \Delta E$ plane. Here, black dots (shaded boxes) express the data (signal MC), the region bounded by two lines is defined as a 5 σ band for the BG estimation and the elliptic region is the signal one which corresponds to 3 σ in each plot. One event is found in the signal region for $\tau \rightarrow \mu K^{*0}$, $\mu\bar{K}^{*0}$ and $\mu\phi$ while no events appear in any other modes.

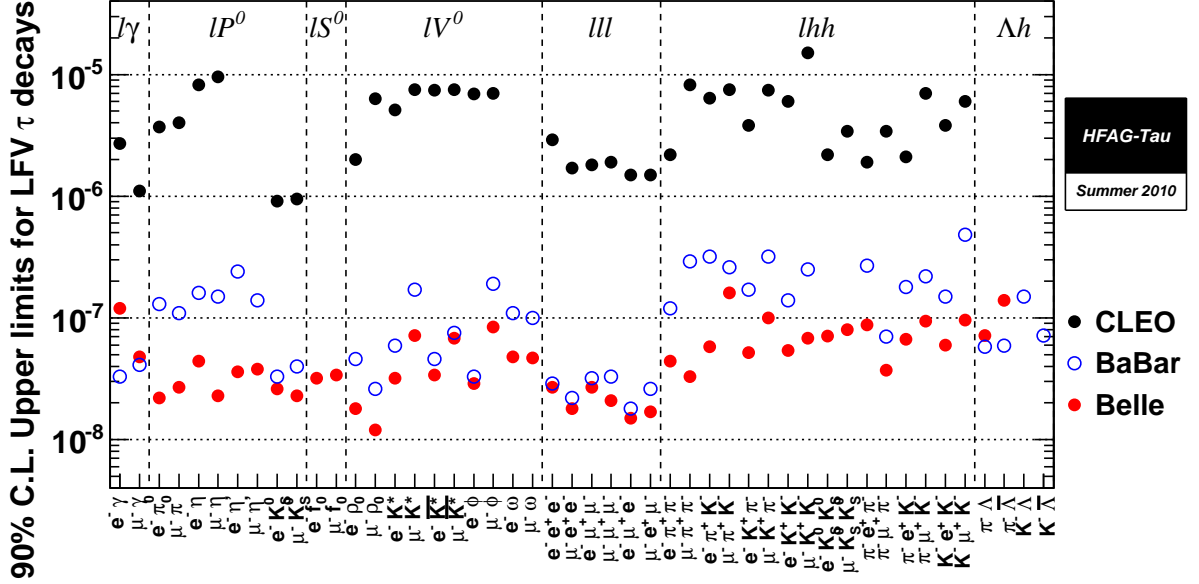


Figure 4. Upper limits on the branching fractions for the LFV τ decays. Here, red, blue and black circles express the results obtained by Belle, BaBar and CLEO, respectively [4].

3. CPV measurement with the τ decay into $\nu K_S^0 \pi$

In SM, CP in the lepton sector is conserved. However, by introducing a new scalar field with a complex coupling constant, CPV can be induced. A charged Higgs in the multi-Higgs-doublet model [5] is one of the candidates for such a scalar field. Here, we discuss the CPV appearing in the $\tau \rightarrow \nu K_S^0 \pi$ decay as an interference between the SM and NP processes [6].

3.1. Analysis method

A hadronic current into $K^0 \pi$ can be written as

$$\begin{aligned} J_\mu &= \langle K^0(q_1) \pi(q_2) | \bar{u} \gamma_\mu s | 0 \rangle \\ &= (q_1 - q_2)^\nu \left(g_{\mu\nu} - \frac{Q_\mu Q_\nu}{Q^2} \right) F_V(Q^2) + Q_\mu F_S(Q^2), \end{aligned} \quad (3)$$

where u and s are spinor fields for a u and s quark, respectively, q_1 and q_2 are 4-momenta for K^0 and π , respectively, F_V (F_S) is a vector (scalar) form factor and $Q^\mu = q_1^\mu + q_2^\mu$. To make the current induce CPV, instead of F_S , we introduce \tilde{F}_S , defined as

$$\tilde{F}_S = F_S + \frac{\eta_S}{m_\tau} F_H, \quad (4)$$

where F_H is a form factor for the charged Higgs, η_S is a complex coupling constant [7]. The size of CPV is proportional to an imaginary part of η_S . From the current, in the hadronic rest frame ($\vec{Q} = \vec{0}$), we can calculate the differential partial width for $\tau \rightarrow \nu K_S^0 \pi$ as

$$\begin{aligned} \frac{d\Gamma(\tau \rightarrow \nu K_S^0 \pi)}{d\omega} &= (\text{CP even terms}) \\ &\quad - 4 \frac{m_\tau}{\sqrt{Q^2}} |\vec{q}_1| \Im(F_V F_H^*) \Im(\eta_S) \cos \psi \cos \beta, \end{aligned} \quad (5)$$

where $\omega = dQ^2 d \cos \theta d\beta$, θ (β) is an opening angle between the direction opposite to the one of the CM system and the one of the hadronic system in the τ rest frame (between the direction of K_S^0 and that for the CM system in the hadronic rest frame), and ψ denotes the angle between the direction of the CM frame and the direction of the τ as seen from the hadronic rest frame.

To extract the CP violating term, we define an asymmetry as

$$A_{\psi\beta}^{CP} = \frac{\int \cos \beta \cos \theta \left(\frac{d\Gamma_{\tau^-}}{d\omega} - \frac{d\Gamma_{\tau^+}}{d\omega} \right) d\omega}{\frac{1}{2} \left(\frac{d\Gamma_{\tau^-}}{dQ^2} + \frac{d\Gamma_{\tau^+}}{dQ^2} \right) dQ^2} \simeq \langle \cos \beta \cos \psi \rangle_{\tau^-} - \langle \cos \beta \cos \psi \rangle_{\tau^+}. \quad (6)$$

Therefore, by measuring the second line, we can evaluate $A_{\psi\beta}^{CP}$ experimentally.

3.2. Result and Discussion

With a 699 fb^{-1} data sample, we obtain around 3×10^5 $\tau \rightarrow \nu K_S^0 \pi$ candidates, where it turns out that 23% of them are BG events by MC study. (See Fig. 5(a).) Using them, $A_{\psi\beta}^{CP}$ is evaluated depending on $\sqrt{Q^2} (\equiv W)$. (See Table 3.2 and Figs. 5(b) and (c).) In the final result, $\gamma - Z$ interference and π^\pm detection asymmetry effects are corrected for and the background subtraction is also performed.

Table 3. CP asymmetry in bins of the hadronic mass W . The first and second errors correspond to statistical and systematic ones, respectively.

	$W \text{ (GeV}/c^2\text{)}$			
	0.625–0.890	0.890–1.110	1.110–1.420	1.420–1.775
$A_{\psi\beta}^{CP}$	$7.9 \pm 3.9 \pm 2.8$	$1.8 \pm 2.1 \pm 1.4$	$-4.6 \pm 7.2 \pm 1.7$	$-2.3 \pm 19.1 \pm 5.5$

Consequently, no CPV is found. From this result, we can evaluate the 90% CL upper limit for $|\Im(\eta_S)|$ varying a constant-strong-interaction-phase difference between F_V and F_S :

$$|\Im(\eta_S)| < (0.012 - 0.026). \quad (7)$$

This result is almost one order of magnitude more restrictive than that previously obtained by CLEO [8], i.e., $|\Im(\eta_S)| < 0.19$.

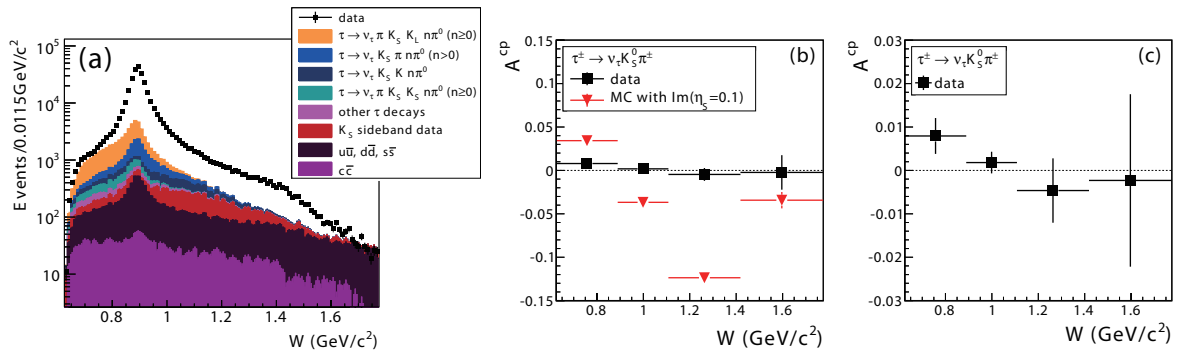


Figure 5. (a) Distribution of W for the $\tau \rightarrow \nu K_S^0 \pi$ candidate, (b) plot for $A_{\psi\beta}^{CP}$ depending on W and (c) zoom of (b).

According to a theoretical prediction for $\Im(\eta_S)$ in the multi-Higgs-doublet model, η_S is written as

$$\eta_S \simeq \frac{m_\tau m_s}{M_{H^\pm}^2} X^* Z, \quad (8)$$

where m_s is an s -quark mass, M_{H^\pm} is the lightest charged Higgs mass, and X and Z are complex constants describing the coupling of the Higgs to the u and s quarks and the τ and ν , respectively. Using the limit $\Im(\eta_S) < 0.026$, we can obtain an inequality:

$$|\Im(XZ^*)| < 0.15 \frac{M_{H^\pm}^2}{1\text{GeV}^2/c^4}. \quad (9)$$

References

- [1] E. Arganda, M. J. Herrero and J. Portoles, JHEP **0806**, 079 (2008).
- [2] G. J. Feldman and R. D. Cousins, Phys. Rev. D **57**, 3873 (1998).
- [3] Y. Miyazaki *et al.* (Belle Collaboration), arXiv:1101.0755 [hep-ex], submitted to Phys. Lett. B.
- [4] It is drawn by HFAG-tau subgroup. You can find it at
<http://www.slac.stanford.edu/xorg/hfag/tau/HFAG-TAU-LFV.htm>
- [5] S. Y. Choi, K. Hagiwara, and M. Tanabashi, Phys. Rev. D **52**, 1614 (1995).
- [6] M. Bischofberger *et al.* (Belle Collaboration), arXiv:1101.0349 [hep-ex] submitted to Phys. Rev. Lett.
- [7] J. H. Kühn and E. Mirkes, Phys. Lett. B **398**, 407 (1997).
- [8] G. Bonvicini *et al.* (CLEO Collaboration), Phys. Rev. Lett. **88**, 111803 (2002).